ELSEVIER

# Tin-filled carbon nanotubes as insertion anode materials for lithium-ion batteries

T. Prem Kumar [a,*], R. Ramesh [a], Y.Y. Lin [b], George Ting-Kuo Fey [b]

[a] *Electrochemical Power Systems Division, Central Electrochemical Research Institute, Karaikudi 630006, Tamil Nadu, India*
[b] *Department of Chemical and Materials Engineering, National Central University, Chung-Li 32054, Taiwan, ROC*

## Abstract

The electrochemical lithium insertion properties of tin-filled multi-walled carbon nanotubes are described. Carbon nanotubes synthesized by the catalytic decomposition method were purified, oxidatively opened, and filled with a tin salt by capillary action. Two methods, an $NaBH_4$-reduction process and a hydrothermal process, were employed to reduce the salt to the metal. Structural characterization of the products was done by X-ray diffraction and transmission electron microscopy. At a 0.1 C rate, the hydrothermally-filled nanotubes gave first-cycle insertion and deinsertion capacities of 1916 and 834 mAh/g, respectively, while the $NaBH_4$-reduced sample gave 2474 and 889 mAh/g. This was much higher than those for the opened carbon nanotubes, which were 1281 and 340 mAh/g, respectively. The reversible capacities of the tin-filled nanotubes were remarkably high, stabilizing in the 720–800 mAh/g region over the first 20 cycles. The electrochemical performance of the materials is correlated with their structural characteristics.
© 2004 Elsevier B.V. All rights reserved.

*Keywords:* Carbon nanotubes; Carbon anodes; Tin-filled carbon nanotubes; Lithium insertion; Lithium-ion battery

## 1. Introduction

Multi-walled carbon nanotubes with their 'Russian doll' model of graphite sheets rolled into concentric cylinders hold much promise for application in lithium-ion battery technology. The spacings between the graphite layers, local turbostratic disorders arising from their highly defective structures, and the central core should permit larger insertion capacities. In fact, studies have shown lithium intake of more than 1400 mAh/g in carbon nanotubes [1–5]. Their irreversible capacities, however, are too large to merit practical applicability. Although other lithium insertion materials such as tin oxides [6–8] and tin-based composite oxides [9–11] have been suggested, their suitability cannot be judged yet. Tin alloys with lithium and has a lithium insertion capacity of 994 mAh/g, corresponding to a composition of Li$_{22}$Sn$_5$ [12]. However, the expansion/contraction associated with the charge–discharge processes leads to a pulverization of the tin anode, which limits its cyclability [13,14].

A recent approach is to use composites of lithium-insertion anode materials. Mention may be made of silver dispersed in carbon [15], Sn–Sb–C composites [16], and pyrolyzed polysiloxanes [17,18]. Sakamoto and Dunn [19] obtained capacities of over 400 mAh/g from a composite of carbon nanotubes with $V_2O_5$ aerogels. According to the authors [19] the aerogel provided electrolyte access into the composite matrix. Liu et al. [20] deposited fine tin particulates on carbonaceous mesophase spherules, and found that the dispersed tin enhanced the reversible lithium insertion capacity. A composite containing 22% tin gave a first-cycle capacity of 428 mAh/g, retaining 91% of the capacity in the 50th cycle [20]. Chen et al. [21], who studied nanocomposites of carbon nanotubes and $Sn_2Sb$ alloys, reported a first cycle insertion capacity of 1250 mAh/g and a deinsertion capacity of 580 mAh/g. In this communication, we

* Corresponding author. Tel.: +91-4565-227550 to 227559; fax: +91-4565-227713/227779.
*E-mail address:* premlibatt@yahoo.com (T. Prem Kumar).

present our results on the lithium insertion behavior of multi-walled carbon nanotubes filled with tin. The carbon nanotubes synthesized by a catalytic decomposition method were purified, oxidatively opened, and filled with a stannous salt by capillary action. The stannous ions were subsequently reduced to the metal.

## 2. Experimental

A substrate of $SiO_2$ was formed on an Si (1 1 0) wafer by oxidation in air at 700 °C for 1 h. Carbon nanotubes were grown on this substrate from ferrocene and acetylene as catalyst and carbon sources, respectively, by a method adapted from the work of Rao and co-workers [22–24]. The substrate and the catalyst particles were removed, respectively, by sonication in 48% HF for 30 min and stirring with 30% $HNO_3$ for 5 h, followed by rinsing in water and drying. The agglomerated bundles of carbon nanotubes were dispersed by sonication in methanol and dried in vacuo. Any amorphous carbon on the nanotubes was removed by heat treatment in a flow of hydrogen at 700 °C for 10 h [25,26]. The oxidative opening of the carbon nanotubes was carried out by treatment with azeotropic $HNO_3$ (68%) for 24 h at 10 °C [27]. The opened nanotubes were then washed with water. Possible surface functional groups like –OH on the nanotubes were removed by a 1-h heat treatment at 900 °C in argon. $SnCl_2$ was introduced into the carbon nanotubes by capillary action by stirring the nanotubes in molten $SnCl_2 \cdot H_2O$ (melting point: 37 °C) at 60 °C for 5 h, such that the weight ratio of carbon:tin was 1:1. The stirred carbon nanotube mass was then rinsed with water, decanted and dried. The reduction of the metallic species sucked into the nanotubes by capillary action was accomplished by two methods. In the first method, hereinafter referred to as the hydrothermal method, the $SnCl_2$-containing dried carbon nanotubes were transferred to a Teflon-lined autoclave. A solution of $Na_2CO_3$ was added to maintain the pH around 7. To this 10 ml of a solution of hydrazine hydrate monohydrate was added. The mixture was autoclaved for 1 h at 150 °C. After cooling, the sample was collected by filtration, washing with water and drying. In the second method, called the $NaBH_4$ reduction method, the dried mass was treated with an excess amount of a 0.1 M solution of $NaBH_4$, washed, filtered and dried.

Powder X-ray diffraction was performed (Siemens D-5000 X-ray diffractometer) with nickel-filtered Cu Kα radiation. The data were collected between scattering angles ($2\theta$) of 5° and 80° in steps of 0.05°. The microstructures of the carbon nanotubes were examined by SEM (Hitachi, model S-3500V) and TEM (JEOL JEM-200FXII). Coin cells of the 2032 configuration were assembled in an argon-filled VAC MO40-1 glove box. The carbon electrodes for the cells were prepared by blade-coating a slurry of 75 wt% carbon nanotubes and 25 wt% PVdF in NMP on a copper foil, followed by drying at 110 °C in an air oven, roller-pressing the dried sheets, and punching out circular discs. The carbon electrode was coupled with lithium metal in the coin cell, with a 1 M solution of $LiPF_6$ in a 1:1 (v/v) mixture of EC-DEC. Galvanostatic charge–discharge profiles were recorded between 3.000 and 0.005 V at 0.1 or 0.3 C rate on a Maccor Series 4000 multi-channel battery tester.

## 3. Results and discussion

The Fe-catalyst tipped carbon nanotube products contained as much as 88.38 wt% of iron, as determined by an ICP-AES analysis. Although the tube ends can be opened by selective oxidation in carbon dioxide [25] or oxygen [26], this treatment can damage the tube walls. An improved method based on nitric acid, described by Tsang et al. [27], was adopted for opening the tubes.

Fig. 1(a) shows the SEM image of the purified carbon nanotubes. The average tube diameters are around 80 nm. TEM images of the tin-filled nanotubes are shown in Fig. 1(b) and (c). Dark patches, indicating deposits of tin, can be noticed. The tin content in the carbon nanotubes, as determined by ICP-AES, were 6.33 and 4.69 wt%, respectively, for the tubes filled by the $NaBH_4$-reduction and the hydrothermal reduction methods. Therefore, although a 1:1 weight ratio of C:Sn was used for the capillary impregnation, only a small percentage of tin found its way into the nanotubes under the conditions employed. Moreover, the metal-filled carbon nanotubes seem to have buckled, with average tube diameters increasing to 150–200 nm. Such bucklings have previously been reported, for example, with $Nd_2O_3$-filled carbon nanotubes [28]. Furthermore, the
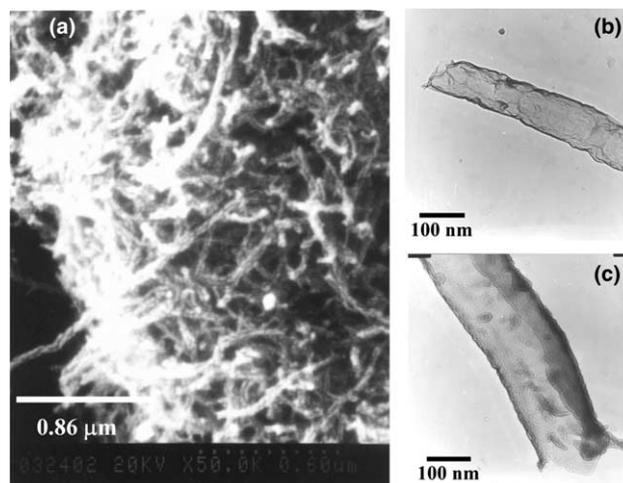


Fig. 1. (a) SEM image of the purified nanotubes and TEM images of the tin-filled carbon nanotubes. (b) Hydrothermal method. (c) $NaBH_4$ method.

average tube diameter in the case of the $NaBH_4$-reduced sample was found to be more than that in the hydro-thermally reduced one ($\sim$100 nm), commensurate with the larger incorporation of tin in the former sample.

According to Chen et al. [28], the two-step filling process involving the opening followed by the capillary filling of the nanotubes normally yields low percentages of fillings. The low metal-filling levels may be attributed to the extra volume occupancy inside the carbon na-notubes by the water molecules in the hydrated stannous chloride as well as by the water ingressing into the na-notubes during the subsequent rinsing step. It was ob-served that the fillings were discrete and scattered, especially in the case of the hydrothermally reduced sample. The distribution of the filler material, either as continuous crystals or in a discontinuous and scattered pattern, depends on the metal and the conditions of the experiment [29,30]. In general, the molten salt filling method is thought to result in a continuous filling [25,28,31]. However, the discrete fillings noted in the $NaBH_4$ reduction method has to do with the dihydrated stannous chloride, which, because of the volume re-quirements of the extra water molecules, results in a diminished filling of the nanotubular space by the metal species. The lower levels of metal filling in the hydro-thermal method may be explained by the exudation of water and tin-containing species from the nanotubes during the hydrothermal process. It may be noted that the more or less uniform filling by the metal in the $NaBH_4$-reduced sample must be attributed to the lower amounts of water that may exude from the nanotubes during the reduction and drying processes.

The X-ray diffractograms of the various carbon nanotube samples are presented in Fig. 2. The as-pre-pared unopened carbon nanotubes show broad, but characteristic $(0\,0\,2)$ and $(1\,0\,0)$ reflections. The intensity of the $(1\,0\,0)$ reflections gets diminished in the oxida-tively opened nanotubes, indicating that the concentric carbon cylindrical structures were damaged and disor-dered. Extra diffraction peaks can be noticed in the XRD patterns of the tin-filled samples. A comparison with the standard X-ray diffraction patterns of Sn and $SnO_2$ shows that the several extra peaks can be assigned to the tin and its oxide formed in the nanotube samples. Additionally, a few minor peaks appearing in the $NaBH_4$-reduced sample may be attributed to the pres-ence of residual boron in the samples formed from the reducing agent.

As noted from our electron microscopic studies, the tin-filled carbon nanotubes had increased average tube diameters, typically between 150 and 200 nm. If part of the metal gets incorporated between the graphite layers, the inter-layer spacings in the tin-filled carbon nanotu-bes should be larger than that in the unfilled sample. The value of the $d_{002}$ spacings in the opened sample was 3.490 Å, while those in the tin-filled samples were
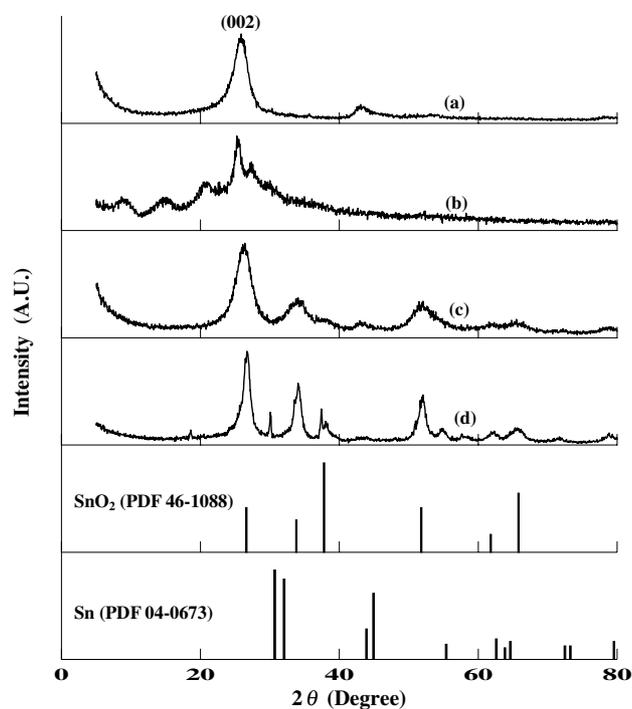


Fig. 2. X-ray diffractograms of the various carbon nanotubes: (a) unopened; (b) opened; (c) tin-filled by $NaBH_4$ reduction; (d) tin-filled by hydrothermal reduction.

3.373 Å ($NaBH_4$-reduced) and 3.336 Å (hydrothermally reduced). The shrinking of the layer spacing is contrary to the observations made with carbon nanotubes filled with $Nd_2O_3$ [28], where inter-layer spacings of 20 Å were reported. However, it is seen that the $d_{002}$ spacing and the nanotube diameter increase with an increase in the amount of metal incorporated.

Galvanostatic cycling was first done at 0.1 C rate with respect to the theoretical capacity of 372 mAh/g of graphite (Fig. 3). It was seen that the unopened carbon nanotubes could insert 808 mAh/g equivalent of lithium in the first cycle. However, only 207 mAh/g could be deinserted. These values compare well with some data reported on lithium insertion in multi-walled carbon nanotubes [32–34]. The corresponding values for the opened structure were 1281 and 340 mAh/g. The en-hanced capacity of the opened nanotubes shows that the number of lithium accommodation sites is considerably more in these structures. In addition to the tube ends, where lithium intercalation at the prismatic surfaces (arm-chair and zig-zag faces, as in graphitic structures) is possible, two more fronts are opened up for increased insertion. One is the open channel, which serves as a one-dimensional conduit for lithium accommodation, and the other is the defect sites on the surface (akin to the basal planes in graphite) [35] through which lithium can penetrate into the carbon structure. In fact, carbon nanotubes have been shown to be highly defective, with local structures similar to turbostratic graphite [36].
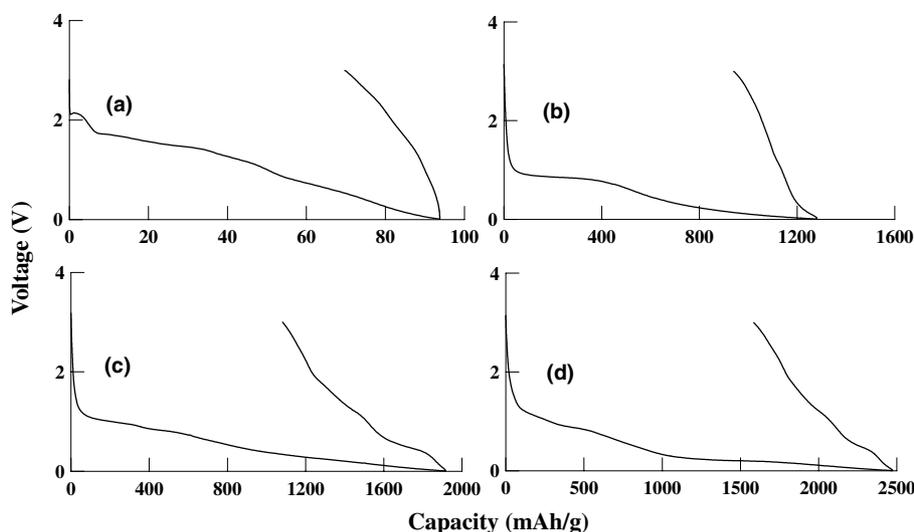
Fig. 3. The first-cycle insertion and deinsertion behavior of the various carbon nanotubular materials: (a) unopened; (b) opened; (c) tin-filled (hydrothermal); (d) tin-filled ($NaBH_4$).

Such surface defects, usually seen as surface lacerations, may be generated during the oxidative tube-opening process. The deinsertion capacity of the unopened nanotubes faded to 170 mAh/g in a matter of 10 cycles. On the contrary, the reversible capacities of the opened nanotubes seemed to stabilize around 320 mAh/g around the 25th cycle, although from then on the capacity increased with the cycling.

The carbon nanotubes filled by the hydrothermal reduction method gave a first-cycle insertion capacity of 1916 mAh/g and a deinsertion capacity of 834 mAh/g. The corresponding values for the carbon nanotubes filled by the $NaBH_4$-reduction method were 2474 and 889 mAh/g. It must be noted that the amount of tin incorporated into the nanotubes has a direct bearing on the capacity characteristics of the tin-filled nanotubes. For comparison, the charge–discharge behavior of an electrode made of nanoparticulate tin was studied. The nanotin had an average particle size of 40–60 nm. The first-cycle insertion and deinsertion capacities of this material were 1035 and 274 mAh/g, respectively. In fact, the first-cycle insertion capacity of the nanotin material exceeds 994 mAh/g, the theoretical value for the $Li_{22}Sn_5$ composition. We speculate that some impurity phase formed with boron during the preparation, which involved the reduction of stannous ions by $NaBH_4$, may be responsible for the excess capacity. It is clear that the first-cycle insertion capacities of the tin-filled nanotubes exceed the cumulative lithium insertion capacities of the individual constituents. It must be recalled that Chen et al. [21] reported capacities that were more than the weighted sum of the specific capacities of the carbon nanotubes and alloys in their study on carbon nanotubes-$Sn_2Sb$ nanocomposites. However, such high capacities are a contrast from the behavior of carbon–tin

composites, which generally give capacities intermediate between those of the constituents [20]. Thus, metal-filled carbon nanotubes are superior electrode materials than are metal-carbon nanotube composites.

The cycling behavior of nanotin, the unopened, opened but unfilled, and the opened and tin-filled nanotubes at 0.1 C rate is given in Fig. 4(a). The fall in capacity with cycling was precipitous in the case of nanotin, falling from 274 mAh/g in the first cycle to 35 mAh/g in the fifth cycle. The unopened carbon nanotubes gave a first-cycle deinsertion capacity of 207 mAh/g, fading to 170 mAh/g in the 10th cycle. Due to the low capacities, the cycling of nanotin and unopened carbon nanotubes was halted. Although high reversible capacities could be obtained with the tin-filled nanotubes, the first-cycle irreversible capacities were high. For example, the first-cycle irreversible capacities of the hydrothermally reduced and $NaBH_4$-reduced products were 1082 and 1585 mAh/g, respectively.

The high irreversible capacities are attributed to loss of lithium due to (1) reaction with surface functional groups [32] that could have been generated during the capillary insertion and subsequent steps, (2) irretrievability of lithium inserted into certain sites in the carbon nanotubes [37], (3) irreversible formation of $Li_2O$ with any residual tin oxide in the nanotubes, and (4) formation of a solid electrolyte interface [38]. The irreversible capacities were considerably reduced as the cycling progressed. Looking at it differently, the coulombic efficiencies in the first cycle for the tin-filled materials were low (44% and 36%, respectively, for the hydrothermally reduced and $NaBH_4$-reduced products), but rose to 98% and 97% in the 40th cycle. As with the opened nanotubes, the reversible capacities of the tin-filled nanotubes also showed an increase with cycling. No immediate
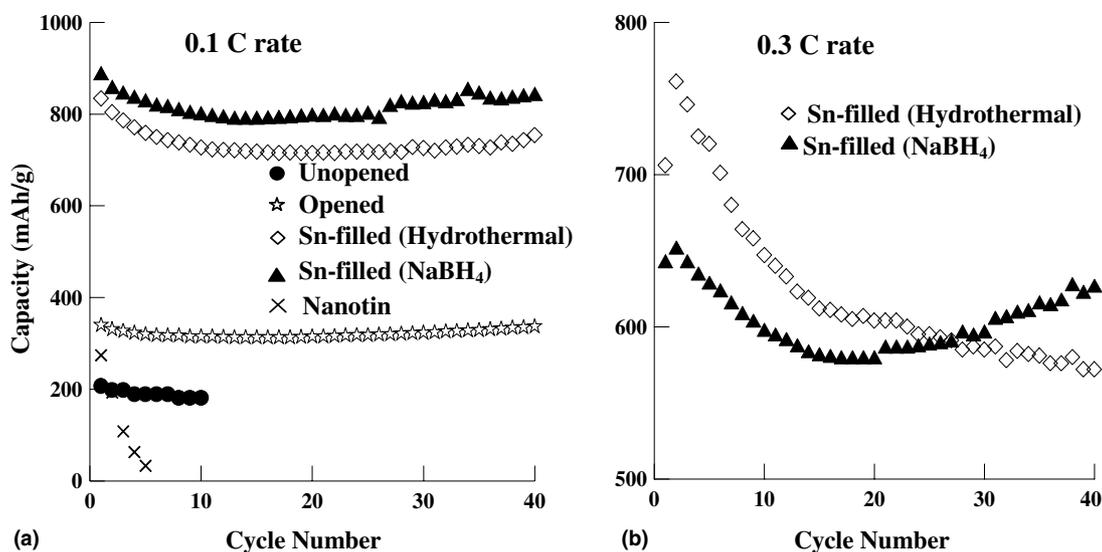
Fig. 4. Cycling behavior of nanotin, the unopened, opened but unfilled, and the tin-filled carbon nanotubes.

explanation for the steady increase in capacity with cycling is forthcoming. It must be mentioned that the 40th-cycle capacities of 754 and 844 mAh/g for the hydrothermally reduced and NaBH$_4$-reduced products, respectively, are remarkably large values for lithium-insertion anode materials. This compares favorably with the results of Chen et al. [21], who reported about 450 mAh/g in the 40th cycle for nanocomposites of carbon nanotubes with 56 wt% Sn$_2$Sb. Moreover, considering the fact that only a small fraction of Sn has been introduced into the carbon nanotubes (4.69 and 6.33 wt% by the hydrothermal and NaBH$_4$-reduction methods, respectively), it is clear that the capacity largely arises from the carbon nanotubular structures.

The tin-filled nantubes were also cycled at 0.3 C rate in order to examine their high-rate performance (Fig. 4(b)). The first-cycle insertion and deinsertion capacities for the hydrothermally reduced product were 1590 and 706 mAh/g, respectively, while the corresponding values for the NaBH$_4$-reduced product were 1729 and 643 mAh/g. It must be noted that although the first-cycle insertion capacities were lower at the higher rate, the irreversible capacities were considerably higher, being 56% and 63%, respectively, for the hydrothermally reduced and the NaBH$_4$-reduced products. Again, what is significant here are the good high-rate capability and the high capacities of the tin-filled nanotubes: The de-insertion capacities of the hydrothermally reduced and NaBH$_4$-reduced products in the 40th cycle were 572 and 627 mAh/g, respectively, the corresponding coulombic efficiencies being 97% and 98%.

Although the capacities are consistent with the extent of tin loading into the nanotubes, the high capacities are not entirely due to the metal. With just 4.69 and 6.33 wt% of tin incorporated, a maximum capacity of only 47 and 63 mAh/g, respectively, can be expected from the

metal inclusions in the hydrothermally reduced and NaBH$_4$-reduced samples. Moreover, the specific charge obtained from the open nanotubes even in the first cycle is only in the vicinity of 340 mAh/g. Thus, the larger capacity of the nanotubes loaded with tin must come from the large number of lithium accommodation sites in the lacerated and turbostratically disordered regions of the carbon nanotubes. It must be noted that not only do the tin-filled nanotubes yield higher capacities, but also cycle better than the unfilled materials.

## 4. Conclusions

Multi-walled carbon nanotubes were oxidatively opened, filled with a stannous salt by capillary action. The stannous ions were reduced by two methods, a hydrothermal reduction process and an NaBH$_4$-reduction process. ICP-AES analysis of the reduced samples indicated that the former sample contained 4.69 wt% of tin, while the latter contained 6.33 wt% of tin. While the first-cycle insertion and deinsertion capacities at a 0.1 C rate for the hydrothermally filled nanotubes were 1916 and 834 mAh/g, respectively, the corresponding values for the NaBH$_4$-reduced sample were 2474 and 889 mAh/g. The reversible capacities of the tin-filled nanotubes were remarkably high, the capacities in the 40th cycle at a 0.1 C rate being 754 and 844 mAh/g, respectively, for the hydrothermally reduced and NaBH$_4$-reduced samples. The high-rate cyclability of the tin-filled materials was also impressive. The capacities of the tin-filled nanotubes far exceeded the cumulative value that may be expected from the constituents. Although the initial irreversible capacities were high (as much as 56% and 67% for the hydrothermally reduced and NaBH$_4$-reduced samples, respectively), the capacity

loss decreased with cycling, being just 2% and 3% in the 40th cycle at the 0.1 C rate.

## References

[1] J.R. Dahn, T. Zheng, Y. Liu, J.S. Xue, Science 270 (1995) 590.
[2] J.C. Withers, R.O. Loufty, J.P. Lowe, Fullerene Sci. Technol. 5 (1997) 1.
[3] V.A. Nalimova, D.F. Skovsky, G.N. Bondarenko, H. Alvergnt-Gaucher, G. Bonamy, F. Beguin, Synth. Met. 88 (1997) 89.
[4] G.T. Wu, C.S. Wang, X.B. Zhang, H.S. Yang, Z.F. Qi, P.M. He, W.Z. Li, J. Electrochem. Soc. 146 (1999) 1698.
[5] T. Prem Kumar, A. Manuel Stephan, P. Thayananth, V. Subramanian, S. Gopukumar, N.G. Renganathan, N. Muniyandi, M. Raghavan, J. Power Sources 97–98 (2001) 118.
[6] I.A. Courtney, J.R. Dahn, J. Electrochem. Soc. 144 (1997) 2943.
[7] W. Liu, X. Huang, Z. Wang, H. Li, L. Chen, J. Electrochem. Soc. 145 (1998) 59.
[8] T. Brousse, R. Retoux, U. Herterich, D.M. Schleich, J. Electrochem. Soc. 145 (1998) 1.
[9] Y. Idota, T. Kubota, A. Matstufuji, Y. Maekawa, T. Miyasaka, Science 276 (1997) 1395.
[10] I.A. Courtney, J.R. Dahn, Prog. Batteries Battery Mater. 16 (1997) 214.
[11] S. Machill, T. Shodai, Y. Sakurai, J. Yamaki, J. Power Sources 73 (1998) 216.
[12] J. Wang, I.D. Raistrick, R.A. Huggins, J. Electrochem. Soc. 133 (1986) 457.
[13] D. Fauteux, R. Koksbang, J. Appl. Electrochem. 23 (1993) 1.
[14] W.C. Maskell, J.R. Owen, J. Electrochem. Soc. 132 (1985) 1602.
[15] J. Aragane, K. Matsui, H. Andoh, S. Suzuki, H. Fukuda, H. Ikeya, K. Kitaba, R. Ishikawa, J. Power Sources 68 (1997) 13.
[16] L.H. Shi, H. Li, W. Lu, X.J. Huang, L.Q. Chen, Proceedings of the Seventh Asian Conference Solid State Ionics, Fuzhou, China, October 29–November 4, 2000, p. 357.
[17] A.M. Wilson, J.R. Dahn, J. Electrochem. Soc. 142 (1995) 326.
[18] W.B. Xing, A.M. Wilson, K. Eguchi, G. Zank, J.R. Dahn, J. Electrochem. Soc. 144 (1997) 2410.
[19] J.S. Sakamoto, B. Dunn, J. Electrochem. Soc. 149 (2002) A26.
[20] Y. Liu, J.Y. Xie, Y. Takeda, J. Yang, J. Appl. Electrochem. 32 (2002) 687.
[21] W.X. Chen, J.Y. Lee, Z. Liu, Electrochem. Commun. 4 (2002) 260.
[22] R. Sen, A. Govindaraj, C.N.R. Rao, Chem. Phys. Lett. 267 (1997) 276.
[23] C.N.R. Rao, R. Sen, B.C. Satishkumar, A. Govindaraj, Chem. Commun. (1998) 1525.
[24] B.C. Satishkumar, A. Govindaraj, C.N.R. Rao, Chem. Phys. Lett. 307 (1999) 158.
[25] S.C. Tsang, P.J.F. Harris, M.L.H. Green, Nature 362 (1993) 520.
[26] P.M. Ajayan, T.W. Ebbesen, T. Ichihashi, S. Ijima, K. Tanigaki, H. Hiura, Nature 362 (1993) 522.
[27] S.C. Tsang, Y.K. Chen, P.J.F. Harris, M.L.H. Green, Nature 372 (1994) 159.
[28] Y.K. Chen, A. Chu, J. Cook, M.L.H. Green, P.J.F. Harris, R. Heesom, M. Humphries, J. Sloan, S.C. Tsang, J.F.C. Turner, J. Mater. Chem. 7 (1997) 545.
[29] C. Guerret-Piecourt, Y. Le Bouar, A. Loiseau, H. Pascard, Nature 372 (1994) 761.
[30] P.M. Ajayan, O. Stephan, P. Redlich, C. Colliex, Nature 375 (1995) 564.
[31] P.M. Ajayan, S. Iijima, Nature 361 (1993) 333.
[32] E. Frackowiak, S. Gautier, H. Gaucher, S. Bonnamy, F. Beguin, Carbon 37 (1999) 61.
[33] B. Gao, A. Kleinhammes, X.P. Tang, C. Bower, L. Fleming, Y. Wu, O. Zhou, Chem. Phys. Lett. 307 (1999) 153.
[34] H.C. Shin, M. Liu, B. Sadanadan, A.M. Rao, J. Power Sources 112 (2002) 216.
[35] T.D. Tran, K. Kinoshita, J. Electroanal. Chem. 386 (1995) 221.
[36] O. Zhou, R.M. Fleming, D.W. Murphy, C.H. Chen, R.C. Haddon, A.P. Ramirez, S.H. Glarum, Science 263 (1994) 1744.
[37] G.T.K. Fey, D.C. Lee, Y.Y. Lin, T. Prem Kumar, Synth. Met. 139 (2003) 71.
[38] D. Aurbach, Y. Ein-Eli, J. Electrochem. Soc. 142 (1995) 1746.